DESIGN STUDY ON HYDROGEN SUPERSONIC TRANSPORT AIRCRAFT ON THE BASIS OF THE CONCORDE

B. Türkyilmaz*, A. E. Scholz*, J.-M. Chrzan*, M. Hornung*
* Technical University of Munich, Chair of Aircraft Design, Boltzmannstraße 15, Garching bei München, Germany

Abstract

A study to assess the feasibility of a supersonic transport aircraft (SST), which is hydrogen-powered, was undertaken. For this purpose, the aircraft design environment Aircraft Design Box (ADEBO) of TU Munich was modified for kerosene and hydrogen SST design. The modifications for the kerosene SST design were validated with the design of a reference aircraft, using the same requirements as the Concorde, which resulted in a close match. Using this reference, a baseline liquid hydrogen-powered SST with as little configurative changes as possible was designed, which led to significant changes on overall aircraft level. Among the changes were a small increase in maximum take-off mass, alongside large increases in operating empty mass, energy consumption in the design mission, and zero-lift drag. The placement of hydrogen tanks inside the fuselage also led to an increase of the fuselage length to over 80 m, which violates airport constraints. To remedy these implications, in a parametric study, a modernized engine was used in the design of the liquid hydrogen-powered SST. Although this engine change significantly reduces the design masses, energy consumption, and fuselage length, its aerodynamic efficiency in cruise decreases in comparison to the baseline hydrogen SST. However, this design shows potential for the improvement of aerodynamic characteristics via configurative changes, such as a new wing planform and fuselage shaping. To fully understand the potential of the aircraft presented in this study, in the future, the evaluation of their sonic boom characteristics and climate impact should be undertaken.

Keywords

Aircraft design; Supersonic transport aircraft; Liquid hydrogen powered aircraft

NOMENCLATURE

Symbols

C_{D0}	Zero-lift drag coefficient	$[-]$
$C_{D0}S_{ref}$	Zero-lift drag area	$[\mathrm{m}]$
C_D	Drag coefficient	$[-]$
C_L	Lift coefficient	$[-]$
$h_{ceiling}$	Service ceiling	$[FL]$
h_{TOC}	Top of climb altitude	$[FL]$
k	Induced drag coefficient	$[-]$
L/D	Lift-to-drag ratio	$[-]$
Ma	Mach number	$[-]$
R	Range	$[\mathrm{km}]$
S_{ref}	Wing reference area	$[\mathrm{m}^2]$
T/W	Thrust-to-weight ratio	$[-]$
V_{stall}	Stall speed	$[\mathrm{m\,s}^{-1}]$
W/S	Wing loading	$[\mathrm{N\,m}^{-2}]$

Abbreviations

AAA	Advanced Aircraft Analysis
ADEBO	Aircraft Design Box
AIAA	American Institute of Aeronautics and Astronautics
ASK	Available Seat Kilometers
ATAG	Air Transport Action Group
AVL	Athena Vortex Lattice
CFRP	Carbon Fiber Reinforced Polymer
FL	Flight Level
FLOPS	Flight Optimization System
IATA	International Air Transport Association
ICAO	International Civil Aviation Organization
LH_2	Liquid Hydrogen
MLM	Maximum landing mass
MPLM	Maximum payload mass
MTOM	Maximum take-off mass
OEM	Operating empty mass
PrADO	Preliminary Design and Optimisation Program
RDS	Raymer's Design System
SST	Supersonic Transport Aircraft
TLAR	Top-Level Aircraft Requirement
TSFC	Thrust-Specific Fuel Consumption

1. INTRODUCTION

The air transport market is expected to grow substantially, even when facing rising energy costs and environmental concerns. The International Air Transport Association (IATA) expects the global passenger travel to return to pre-pandemic levels by 2024 and continue its growth by 3.3% per year afterwards, reaching 8 billion passenger journeys per year by 2040 [1]. The Air Transport Action Group (ATAG) and the International Civil Aviation Organization (ICAO) have both set goals for their members to achieve net zero CO_2-emissions in aviation by 2050 [2, 3]. Since a supersonic transport aircraft (SST) offers a considerable reduction in flight times compared to subsonic aircraft, the number of available seat kilometers (ASK) in a fixed time period can be increased. A hydrogen-powered SST combines the opportunity of increasing the total ASK with CO_2-neutral flight, addressing both issues simultaneously. Evaluating the potential of such an aircraft requires the consideration of phenomena exclusive to supersonic flight, such as supersonic wave drag. Therefore, the aircraft design environment of the Chair of Aircraft Design at the

doi: 10.25967/610166

Technical University of Munich, which is called the Aircraft Design Box (ADEBO) [4], will be extended with methods for supersonic transport aircraft design. This paper introduces the implementation of changes in ADEBO for kerosene and liquid hydrogen (LH_2) SST design. Using these changes, the feasibility of an LH_2 SST on the basis of the Concorde is examined and discussed.

2. STATE OF THE ART ON SUPERSONIC & HYDROGEN AIRCRAFT DESIGN

Designing an SST is not a new endeavor. Multiple programs were conducted in the past, resulting in two production aircraft. These efforts are summarized in Section 2.1. A short overview of previous research efforts into hydrogen propulsion in SSTs is presented in Section 2.2. Known aircraft design environments for SST design are introduced in Section 2.3.

2.1. Previous Kerosene SST Programs

In the 20th century, multiple SST programs were launched with different range, payload, and cruise speed requirements. The most well-known of these programs is the partnership between Britain and France, which resulted in the Concorde. This cooperation resulted from the two nations working independently on similar aircraft concepts with comparable requirements, therefore deciding to merge their efforts. The Concorde had a cruise Mach number of 2.02 and entered service in 1976. The USA also conducted their own evaluation of multiple SST designs with different ranges and speeds, deciding on a Boeing design with a cruise speed of Mach 2.7 with variable sweep wings. This program underwent many changes, such as the replacement of the variable sweep wing with a delta wing. In spite of these efforts, this program was canceled in 1971. The USSR designed and built the Tupolev TU-144, which had distinct features such as retractable canards improving low flight speed characteristics, low-bypass turbofans, and no wing twist. However, the inability of this aircraft to cruise in supersonic speeds without using its afterburners led to high operating costs. After 1983, it was withdrawn from service. [5]

2.2. Previous Hydrogen SST Studies

Studies on supersonic hydrogen-driven aircraft have been conducted for many decades. In this section five representative studies will be presented. One of the first research on hydrogen SSTs was conducted by Brewer in 1974. The study was subdivided into two phases: In the first phase, Brewer conducted a parameter analysis to identify a preferred configuration. This configuration was then investigated in more detail in the second phase. A structural basic design, the cryogenic fuel tanks, and a thermal protection system were established. The design requirements were a cruise Mach number of 2.7, a range of $4,200$ NM, and a payload of $22,226$ kg, which corresponds to 234 passengers. For the trade-off investigations, a kerosene SST with the same design criteria was used as the baseline. The focus of the trade-off studies was on the environmental assessment in relation to noise, sonic boom overpressure, and exhaust emissions, besides the cost and the energy demand per seat mile. [6]
Further research on hydrogen-driven supersonic aircraft concepts was conducted at the University of Tokyo. Yuhara and Rinoie published different concepts. The first three concepts had a design Mach number of 1.6. In the study of 2010, a comparison of a kerosene and a hydrogen SST for a design range of $3,500$ NM and 60 passengers was presented. In addition, an investigation of a double-bubble fuselage configuration was conducted. With a design range of $6,000$ NM and a payload of 100 passengers, a baseline concept (kerosene-fueled) and an LH_2-fueled SST were designed. A special focus was put on the investigation of the use of hydrogen to reduce the sonic boom level. In 2012, a second study was published with a design range of $3,500$ NM and a payload of 50 passengers. The feasibility of an LH_2-powered SST was shown with the help of a multi-point optimization. The aim of the optimization was, among others, to minimize the sonic boom in order to achieve a low-boom vehicle. Two years later, a study with the focus on the performance and environmental impacts of LH_2 SST concepts was conducted. A comparison to a kerosene-fueled aircraft regarding the performance, climate changes, the sonic boom, NO_x emissions, and airport noise was executed. [7–11]

2.3. Aircraft Design Environments for SST Design

Conceptual aircraft design is iterative in nature, involving many different design disciplines (e.g., aerodynamics, propulsion, structures, etc.). This is why computer programs for conceptual aircraft design have been developed, combining the analysis methods of the different disciplines, facilitating the work of the design engineer. Amongst the most well-known aircraft design environments in research are the Flight Optimization System (FLOPS) by NASA from 1984 and the more recent open-source program SUAVE by Stanford University (2017). Both are capable of designing subsonic as well as supersonic civil transport aircraft as they provide methods for supersonic aerodynamic calculation [12, 13]. Furthermore, optimization algorithms are included. In Germany, the Preliminary Design and Optimisation Program (PrADO) and its supersonic extension PrADO-Sup were developed at Technical University of Braunschweig in the 1990s [14, 15]. It includes a grid generator and the higher order panel code HISSS [16] for supersonic aerodynamic handling. Commercial aircraft design environments capable of supersonic aircraft design are, among others, Raymer's Design System (RDS) and Advanced Aircraft Analysis (AAA) based on the methods described in the books by Raymer and Roskam [17, 18].

3. METHODOLOGY

In this section, the methodology used to conduct the design study for an LH_2 SST is described. As a starting point, the aircraft design environment ADEBO, its working principles, and a subsonic transport aircraft design schedule is introduced in Section 3.1. This subsonic schedule is then extended with the required calculation methods for an SST design, which are further explained in Section 3.2. This resulting SST design schedule is then used to design an SST with the same top-level aircraft requirements (TLARs) and aircraft configuration, in order to validate the used methodology. This aircraft is introduced and compared to the Concorde in Section 4.1. As the next step, the SST design schedule is modified to use LH_2 as the energy source, which is further explained in Section 3.3. With as few configurative changes as possible to enable the comparison with the kerosene variant, a baseline LH_2 SST is then designed using this schedule with the same TLARs. The resulting baseline LH_2 SST is presented in Section 4.2.

3.1. ADEBO and Subsonic Transport Aircraft Design Schedule

Within this work, the aircraft design are undertaken using the aircraft design environment ADEBO [4]. This Matlab-based environment is under development at TU Munich and is intended for the design of fixed-wing aircraft configurations of various classes. This includes subsonic civil transport aircraft, unmanned aerial vehicles, and fighter aircraft. It is based on an object-oriented aircraft data model allowing flexible and modular extension. Besides in-house design methods and tools, also interfaces to external programs such as, e.g., the aerodynamic analysis program Athena Vortex Lattice (AVL) by Drela [19] exist. For a more detailed overview of ADEBO the reader is referred to [4].
The subsonic transport aircraft design schedule used as a baseline for the extension to SST design capabilities, mainly follows the methodology outlined by [4] with small adaptations. A flowchart of the schedule is shown in Appendix A.1. At first, TLARs and initial assumptions need to be defined in job 1. In the next job, the fuselage is designed based on the number of passengers to be carried and the class layout. Then, basic aerodynamic figures are estimated with handbook methods (job 3) to enable the point performance determination in the next step. With the help of a constraint diagram, the required thrust-to-weight ratio and wing loading for the design are evaluated. Using an initial estimate of the maximum take-off mass (MTOM), this allows to calculate the wing area and the sea level thrust. The mission performance module (job 5) then makes use of the fuel fraction method and operating empty mass (OEM) regression by [18] to estimate the fuel mass and OEM. The aircraft's MTOM is updated and iterated within the first iteration loop. After convergence, the turbofan sizing is undertaken in job 6 and the previous calculations are repeated with an updated thrust-specific fuel consumption (TSFC) until convergence is reached. Thereafter, the wing and tail are sized in jobs 6 and 7. Component masses are determined using handbook methods, e.g., by [20, 21] and the positioning of the wing and fuselage group is adjusted to meet a defined relative center of gravity position of the empty aircraft in job 10. With this information, the OEM is updated and the configuration aerodynamics are calculated in the last job. This is done by combining the vortex lattice program AVL, the zero-lift drag component build-up method by [17] and the transsonic wave drag estimation by Malone and Mason [22]. At last, the overall iteration loop is then triggered until the MTOM is converged. During post-processing, the TLARs are checked and a detailed design report is generated.

3.2. Kerosene SST Design Schedule

In this section, the changes made to the subsonic design schedule in ADEBO for the kerosene-powered SST design capability are introduced. These changes were made with the goal of designing a kerosene-powered SST with the same TLARs and overall configuration as the Concorde. Therefore, the design mission and the TLARs which were used are presented, afterwards the required changes are presented for each job. A flowchart of the final SST design schedule can be found in Appendix A.1.

3.2.1. Job 1: TLARs, Design Mission, Assumptions

Alongside updating the initial assumptions, such as the maximum take-off mass (MTOM) or the wing reference area (S_{ref}) at the beginning of the design process with Concorde values, the wing and vertical tail shapes are modeled with more detail compared to the subsonic schedule. This is required because the aerodynamic calculations in the supersonic flow regime require more specific geometric descriptions of these surfaces compared to the reference subsonic design schedule. Since a high number of partitions would be needed to approximate an ogee curved-wing in ADEBO (the leading and trailing edges of a partition can only be linear), the wing and vertical tail are approximated as cropped double-delta wings. An illustration showing the approximated geometry is shown in FIG 1.

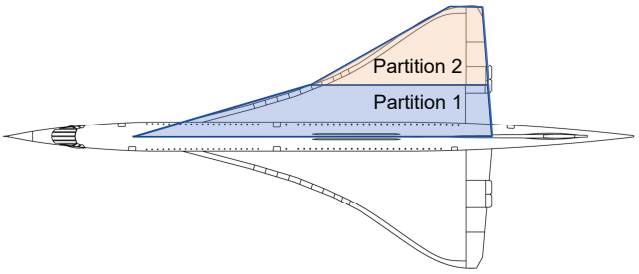

FIG 1. Wing geometry approximation

A list of some of the assumptions and TLARs used for the Concorde re-design can be found in TAB 1.

TAB 1. Assumptions and TLARs for the Concorde re-design

Description	Parameter	Value	Source
Maximum take-off mass	MTOM	$185,070$ kg	[23, p. 14]
Maximum payload mass	MPLM	$12,700$ kg	[23, p. 14]
Maximum landing mass	MLM	$111,130$ kg	[24, p. 1.1.16]
Cruise Mach number	Ma_{cruise}	2.02	[23, p. 14]
Top of climb altitude	h_{TOC}	$FL520$	Own calculation
Service ceiling	$h_{ceiling}$	$FL600$	[25]
Range with max. payload	R	$6,230$ km	[23, p. 14]
Stall speed	V_{stall}	65.3 m s^{-1}	[25]

FIG 2 shows the design mission used for the reference kerosene SST.

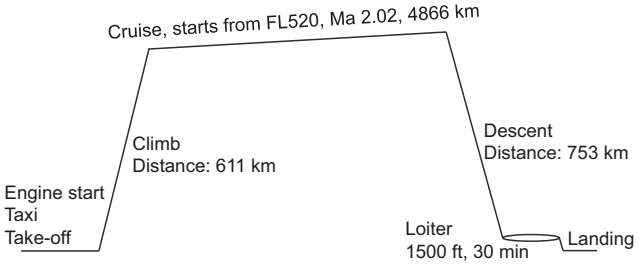

FIG 2. Concorde design mission profile

The climb and descent distances in the design mission are calculated using the rates of climb and Mach numbers available from Eurocontrol [25]. Subsequently, these distances are subtracted from the design range to yield the cruise distance. The top-of-climb altitude is determined to be $FL520$, so as to result in the service ceiling of $FL600$ at the end of cruise.

3.2.2. Job 2: Fuselage Sizing

For the fuselage sizing, the methodology developed by Howe [26] based on the cabin layout and number of passengers is used. This method was already previously

available in ADEBO, only the specific values for SSTs mentioned by Howe are implemented. The fuselage shape is modeled as a cylinder between two Von Kármán ogives for the nose and tail.

3.2.3. Job 3: Basic Aerodynamics

The basic aerodynamics calculation was modified considerably, since the existing functions had to be complemented with methods to estimate aerodynamic characteristics in the supersonic flow regime. The zero-lift drag (C_{D0}) and induced drag (k) coefficients in the supersonic flow regime are calculated with methods based on Torenbeek [27, Ch. 7]. The zero-lift drag in the subsonic regime is calculated with an equivalent skin friction method based on Roskam [28] and Raymer [17], which was already available in ADEBO. The induced drag coefficient k in subsonic flight is calculated using a method by Nita & Scholz [29], which allows for the estimation of the Oswald factor using geometric parameters. Additionally, the lift curve slope estimations in the subsonic and supersonic regimes are conducted with a method developed for cranked delta wings by Paniszczyn [30].

3.2.4. Job 4: Point Performance

The next step in the design schedule is to determine the wing loading (W/S) and thrust-to-weight ratio (T/W) of the aircraft using previously determined point performance criteria. Although some criteria such as the service ceiling and maximum airspeed are known, the maneuvering masses at those points are unknown. Therefore, these unknown masses are adapted to obtain the known W/S and T/W values of the Concorde.

3.2.5. Job 5: Mission Performance

The mission performance calculation is performed using a slightly altered version of the method used in the subsonic design schedule, to account for the supersonic drag coefficients calculated in the basic aerodynamics calculation. This method from [18] requires energy fractions for all mission phases except cruise and loiter. The energy fractions of the cruise and loiter phases are calculated using Breguet's range and endurance equations.
The mission fuel mass breakdown by [31] is used to determine the relationship between trip fuel and contingency fuel. A further 5% of the trip fuel as final reserves [32] is added to the sum of trip, loiter, and contingency fuel to obtain the total fuel mass.
Using the total fuel mass and the design payload, the operating empty mass (OEM) is determined using a regression method with factors for supersonic civil aircraft described by Roskam [18].

3.2.6. Job 6: Engine Sizing

Since the goal of this study is to design an SST with no configurative changes compared to the Concorde, and engine data from the Olympus 593 engines are available, the Olympus 593 data for the rubber engine sizing with a method described by Nikolai & Carichner [33, p. 469] are used. The thrust and thrust-specific fuel consumption (TSFC) maps for the engines are then created using a method by Howe [26].

3.2.7. Job 7: Wing Sizing

In comparison to the subsonic design schedule, this job is modified to only calculate the internal fuel tank volume, since the wing planform was previously defined during job 1 and the wing area was defined during job 4.

3.2.8. Job 8: Tail Sizing

The vertical tail volume is updated to the value stated by Roskam [28, p. 204] for the Concorde, along with the removal of the horizontal tail sizing algorithm. The tail area is determined using the vertical tail volume and the lever arm, obtained by positioning the trailing edge of the tail in the aft of the fuselage. Since the tail area and the positioning changes each time the lever arm is changed, this calculation is iterated until convergence is reached.

3.2.9. Job 9: Component Mass Estimation

This job required significant changes for an SST design, since the structural elements and systems of an SST differ considerably compared to a subsonic transport aircraft. Since it was not possible to identify a single methodology for all structural and systems masses, the components were divided into a structures group and a systems group. The goal was to use a single methodology for each group to stay consistent with the mass estimation.
For the structures group, the mass estimation methods for the wing, fuselage, and vertical tail described by Howe [26] are used, because they are deemed the most suitable for an SST design. For the systems group, mostly methods described by Torenbeek [20] were used with two exceptions: 1) Paint mass is determined by a method described by Roskam [28], since Torenbeek does not offer a paint mass estimation method. 2) A method specific to SSTs for the air conditioning and pressurization system is available from Howe [26], therefore this method is used.

3.2.10. Job 10: Positions and CG

The desired empty center of gravity location is updated to 52% of the root chord for the Concorde [34]. Otherwise, the wing positioning algorithm is not changed compared to the subsonic schedule.

3.2.11. Job 11: Configuration Aerodynamics

As with the basic aerodynamics calculation, the more detailed configuration aerodynamics calculation also had to be updated for the supersonic flow regime and the peculiarities of an SST design. For the zero-lift drag calculation in the subsonic flow regime, the parasite drag calculation function of OpenVSP [35] was used, complemented by interference drag increments specified by Raymer [17, p. 425].
The zero-lift drag in the supersonic regime is calculated in two steps: the friction drag and wave drag. The friction drag is calculated in the same way as in job 3 (basic aerodynamics), however on the more detailed component level rather than on the whole aircraft level. The wave drag calculation is performed via OpenVSP [36], using an implementation of the method described by Harris [37].
The lift and induced drag characteristics of the whole configuration are calculated using a method developed by Staudacher [38], which is available in ADEBO and is applicable to both the subsonic and supersonic flow regimes (for further information see [39]).
The aerodynamic center of the configuration in subsonic and supersonic flight is estimated with an empirical method from the DATCOM [40].

3.3. LH_2 SST Design Schedule

In this section, the changes performed to the kerosene SST design schedule to enable the use of hydrogen as energy source are explained. The overall logic of the design schedule is kept the same in general except for one change: The fuselage design job (job 2) is moved into the iterative calculation loop. Since the LH_2 tanks cannot be stored inside the thin wings (required for favorable flight performance in supersonic flight), they have to be placed inside the fuselage. Thus, the fuselage needs to be re-sized in each iteration. The job to calculate fuel tank volume inside the wings (job 7) is therefore removed. A flowchart of the LH_2 SST design schedule is shown in Appendix A.1.

3.3.1. Job 1: TLARs, Design Mission, Assumptions

This job is largely unchanged, since the TLARs and the design mission are the same as for the kerosene SST. The assumed TSFC of the Olympus 593 engines is divided by a factor of 2.807, because of the smaller lower heating value of kerosene in comparison to LH_2 [41, 42].

3.3.2. Job 2: Fuselage Sizing

The fuselage sizing job is changed significantly, because the LH_2 tank sizing also takes place in this job. The LH_2 tanks are sized using an in-house tank sizing method [43] based on Brewer [44] and Steiner [45]. The high surface temperature in supersonic flight was accounted for by sizing the insulation layer of the LH_2 tanks using the maximum stagnation temperature for the Concorde ($130\ ^\circ$C, [46]) as the outer temperature. A layout of four LH_2 tanks was used, with two of them in the nose and the other two in the tail. All tanks are non-integral and conically shaped to maximize the volume usage inside the nose and tail. The tank layout

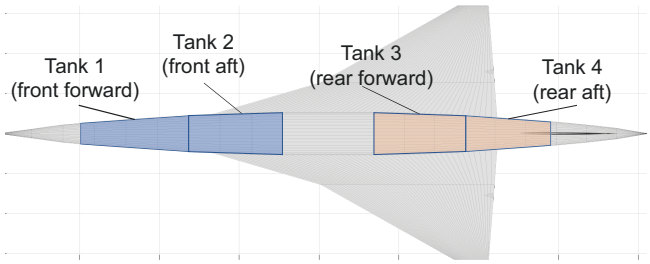

FIG 3. Tank layout for an LH_2 SST

The volume required for the LH_2 tanks is very large. To minimize a fuselage length increase, the cabin is changed from a single-deck to a double-deck, allowing for a larger fuselage diameter. An LH_2 SST design by Brewer [6] is used as a reference point for the double-deck cabin definition. The fuselage diameter is calculated using the number of seats in a row in the upper and lower decks defining the upper and lower deck widths. An illustration of the double-decker cabin can be found in FIG 4.

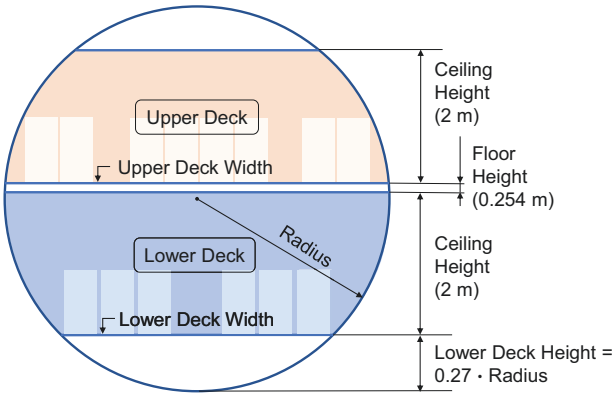

FIG 4. Double-deck cabin layout for an LH_2 SST

Job 3 (basic aerodynamic calculation) was not changed in comparison to the kerosene SST design schedule.

3.3.3. Job 4: Point Performance

In the point performance calculation, the manuevering mass for each requirement is updated for the more lightweight LH_2 as the energy source. Because the assumed manuevering masses are specified as fractions of MTOM and less fuel mass compared to kerosene is burned in flight, these manuevering mass fractions need to increase for an LH_2 SST. A new design point for the LH_2 SST is also needed to keep the same approach speed as the kerosene SST. For this reason, the wing loading of the kerosene SST in approach conditions ($3000\ \mathrm{N\,m^{-2}}$) is set as the target value for the LH_2 SST in approach. However, since the point performance job calculates the required wing loading at maximum take-off mass, this wing loading had to be scaled for the maximum take-off mass using an assumed-mass-at-approach-to-MTOM ratio, which was set at 81.4%. Therefore, the desired wing loading at maximum take-off mass for the LH_2 SST is determined to $3688\ \mathrm{N\,m^{-2}}$. Small deviations of this value are deemed to be acceptable for this study.

3.3.4. Job 5: Mission Performance

The methodology to calculate the mission performance is not changed compared to the kerosene SST design schedule. However, the coefficients for the OEM regression are changed using data from previous LH_2 SST design studies. The regression line is illustrated in FIG 5.

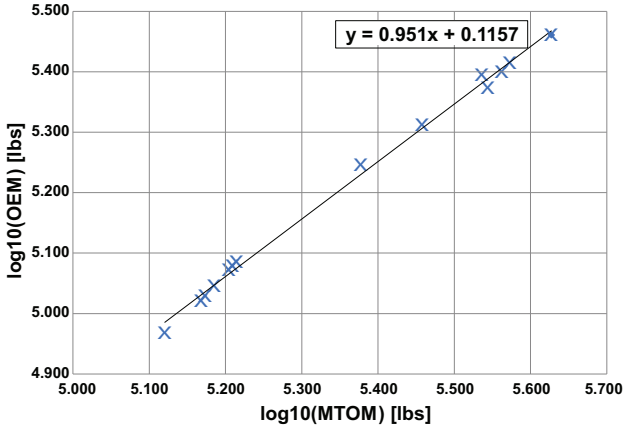

FIG 5. OEM regression line for LH_2 SSTs based on data from previous LH_2 SST design studies [7–9, 11, 47]

3.3.5. Job 6: Engine Sizing

This job is only modified with the scaling factor for TSFC between kerosene and LH_2 previously mentioned in Section 3.3.1.
Job 7 (tail sizing) was not changed compared to the kerosene SST design schedule.

3.3.6. Job 8: Component Mass Estimation

The component mass estimation is changed to account for the impact of using LH_2 as an energy source. Multiple parts of the aircraft are impacted by this change, such as the fuselage and the wing, as well as propulsion and fuel systems.
The masses of the LH_2 tanks are calculated using the previously mentioned tank sizing method by [43] based on Brewer [44] and Steiner [45]. The fuselage mass calculation is split into two calculations, separating the pressurized and unpressurized sections. The pressurized section consists of the cabin and the cockpit. The rest of the fuselage is assumed to be unpressurized. The surface areas of the pressurized and unpressurized sections are computed and used to calculate the respective masses using the method by Howe [26].
Some mass penalties are applied to reflect the need of additional stiffening or isolation in different components and systems, such as the support structure for the LH_2 tanks, double-deck cabin, extra pressure bulkheads and insulation for the fuel lines. The fuselage mass is increased by 6%, the wing mass also by 6%, and the fuel system mass is increased by 80% [44].
The propulsion system mass estimation method by Torenbeek, which was used in the kerosene SST design schedule, also included the fuel tank masses, which is redundant for an LH_2 study. For this reason, an alternative method by Raymer [17] is used. Additionally, the furnishing mass estimation method by Torenbeek also had to be replaced, since the increase in operating empty mass caused by the conversion to LH_2 as the energy source, led to large increases in furnishing mass for the same cabin. Therefore, an alternative method by Howe [26] is used.
Jobs 9 (positions and CG) and 10 (configuration aerodynamics) were not changed compared to the kerosene SST design schedule.

4. RESULTS & DISCUSSION

In this section, the results from the design schedules introduced in Sections 3.2 and 3.3 are presented and discussed. In Section 4.1, the SST design schedule is validated with a Concorde re-design and a comparison of the results with published Concorde data. Afterwards, the Concorde re-design is used as a baseline to design an LH_2 SST, which is presented in Section 4.2. An LH_2 SST with new engines is presented in Section 4.3 as a parametric study.

4.1. Kerosene SST

The main goal of the kerosene SST design was to validate the calculation methods and overall design schedule logic, using an aircraft with a well-established dataset for comparison. The Concorde was selected as the reference aircraft for this purpose. TAB 2 shows a comparison of selected values between the kerosene SST designed in ADEBO and the Concorde.

TAB 2. Comparison of selected aircraft parameters between the kerosene SST and published Concorde values [23, 48]

Name	Kerosene SST	Concorde	Change
MTOM [kg]	$185,660$	$185,070$	$<1\%$
OEM [kg]	$77,589$	$78,700$	-2%
MLM [kg]	$111,489$	$111,130$	$<1\%$
S_{ref} [m^2]	360	358	$<1\%$
Fuselage length [m]	59.5	61.6	-4%
C_{D0} in cruise [-]	0.0111	0.0117	-5%
L/D in cruise [-]	6.99	7.00	$<1\%$
W/S at take-off [N m^{-2}]	$5,063$	$5,071$	$<1\%$
T/W at take-off [-]	0.365	0.37	-2%

In FIG 6, a comparison of top and side views of the kerosene SST designed in ADEBO and the Concorde is shown. The black outline represents the Concorde, whereas the gray areas represent the kerosene SST designed in ADEBO.

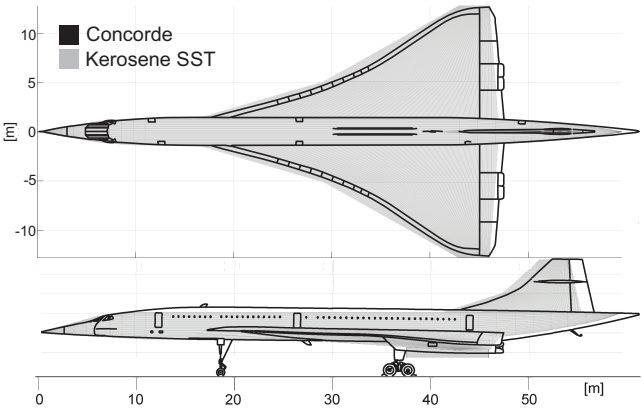

FIG 6. Comparison of top and side views of Concorde and kerosene SST

The shown values of the kerosene SST closely match the values of the Concorde. Small discrepancies exist in operating empty mass and the zero-lift drag in cruise. The reason for these deviations is likely to be the fuselage length, which is 2.1 m shorter compared to the Concorde, as can be seen in FIG 6. Since the goal of this study was to validate the used calculation methodologies, and not to calibrate them to an existing aircraft, this deviation of the conceptual designs was acceptable. The wing and tail positions, which are slightly more forward than those of the Concorde, are also affected by the fuselage length being shorter.
A detailed comparison of the component masses between both aircraft is shown in FIG 7.

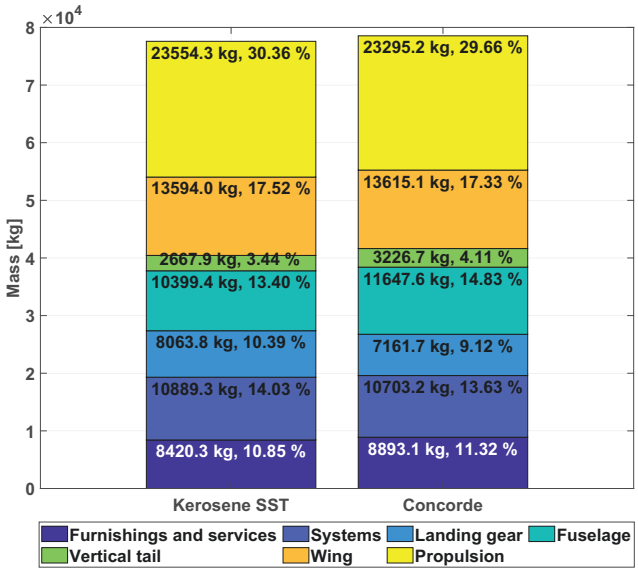

FIG 7. Comparison of component masses between the kerosene SST and published Concorde data from [5]

Some more minor discrepancies can be observed here, such as the fuselage mass. Since the fuselage is 2.1 m shorter than the Concorde, this is reflected also in the fuselage mass, which is around $1,200$ kg lower. Nevertheless, the calculation results with respect to the orders of magnitude for all components were found to be acceptable for this conceptual design study.
Besides the component weights, also the supersonic aerodynamics can be determined very well with the implemented methodology: The kerosene SST drag polar as calculated by ADEBO, matches the published Concorde drag polar in [48] (see FIG 8).

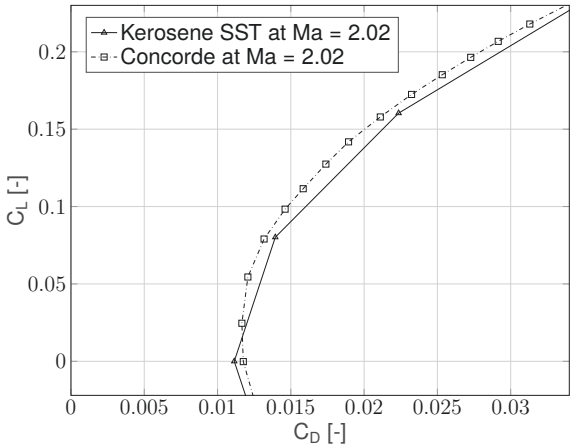

FIG 8. Drag polars of kerosene SST and the Concorde [48]

The characteristic of the published Concorde polar over the C_L range is matched well by the kerosene SST calculated data. As previously mentioned, the zero-lift drag is slightly underestimated. One possible reason for this could be the fuselage length underestimation.
In conclusion, the methods implemented in the kerosene SST design schedule were deemed satisfactory in their accuracy of predicting characteristics and sizing components. More data on the kerosene SST can be found in Appendix A.2.

4.2. Baseline LH_2 SST

In this section, the baseline LH_2 SST, which was designed with as little configurative changes as possible compared to the kerosene SST, is introduced. As previously mentioned in Section 3.3, some configurative changes were necessary, such as a double-deck cabin instead of a single-deck cabin. Nevertheless, the LH_2 SST was designed to the previously mentioned wing loading to keep the same low speed performance, while determining the thrust-to-weight ratio according to the TLARs to keep the same high-speed performance. Therefore, the comparability between kerosene and LH_2 SSTs is ensured.
A comparison of selected aircraft parameters between the kerosene and LH_2 SSTs is shown in TAB 3.

TAB 3. Comparison of selected aircraft parameters between the kerosene SST and baseline LH_2 SST

Name	Kerosene SST	Baseline LH_2 SST	Change
MTOM [kg]	$185,660$	$189,434$	2%
OEM [kg]	$77,589$	$132,083$	70%
MLM [kg]	$111,489$	$157,230$	41%
S_{ref} [m^2]	360	511	42%
Fuselage length [m]	59.5	89.0	50%
C_{D0} in cruise [-]	0.0111	0.0125	13%
L/D in cruise [-]	6.99	6.51	-7%
Trip fuel [kg]	$76,474$	$35,591$	-53%
Trip energy [MJ]	$3.30 \cdot 10^9$	$4.27 \cdot 10^9$	29%
W/S at take-off [N m^{-2}]	$5,063$	$3,637$	-28%
T/W at take-off [-]	0.365	0.570	56%

Using LH_2 as the primary energy source leads to significant changes in key aircraft parameters. The OEM increases by 70%, leading to an increase of 41% in maximum landing mass. The reduction of fuel mass by 53% is insufficient for a reduction in MTOM, which increases by 2%. The overall higher mass of the baseline LH_2 SST, as well as the reduced lift-to-drag ratio (L/D) lead to an increase in the energy consumption during the design mission by 29%. This increase in drag is caused by the overall larger dimensions and the resulting increase in parasitic drag, as well as wave drag due to volume. Another important value is the fuselage length, which increases by 50% to $89\ m$, therefore being larger than the maximum length of 80 m required for airport operations. From the visual comparison of both aircraft (see FIG 9) it can be seen that the aircraft dimensions increase substantially. The wing loading requirement for the LH_2 SST causes a significant increase of 42% in wing area. The fuselage is also significantly larger to accommodate the large LH_2 tanks. The vertical tail is smaller in the baseline LH_2 SST, since the available lever arm is larger and the tail volume is kept the same.

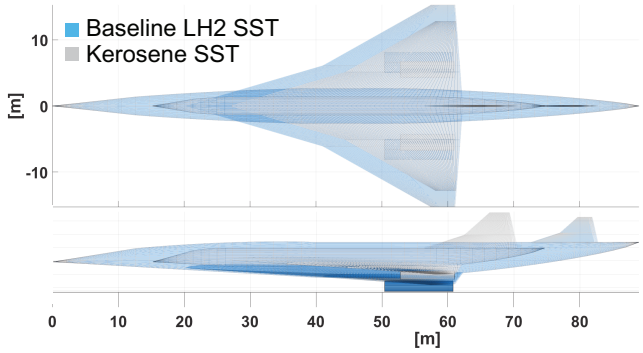

FIG 9. Comparison of top and side views of kerosene and baseline LH_2 SSTs

FIG 10 provides a comparison of the component masses of the two aircraft.

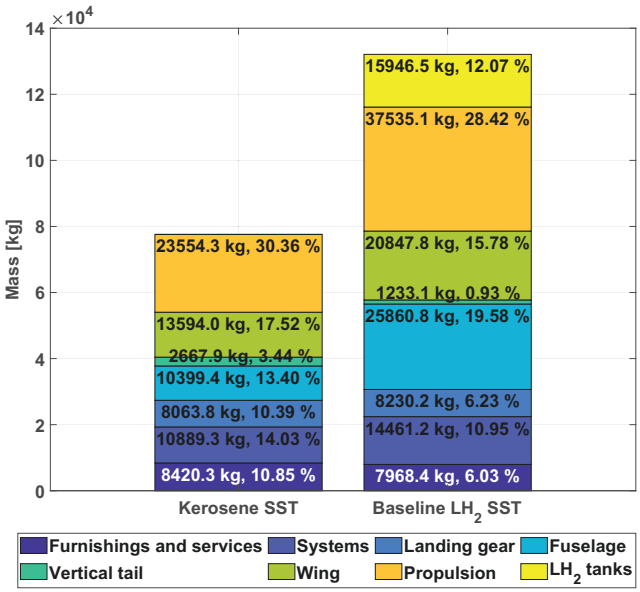

FIG 10. Comparison of component masses between kerosene and baseline LH_2 SSTs

The increase in the overall aircraft dimensions, as well as OEM and MLM lead to an increase in almost all component masses. The mass penalties applied to the wing and fuselage structures alongside the propulsion system mass for the conversion to LH_2 as the primary energy source also play a role in this increase. The LH_2 tanks, which were not included in the kerosene SST, also contribute significantly (12.07%) to the OEM. The vertical tail mass decreases in the baseline LH_2 SST, consistent with its smaller area. The furnishings mass decreases slightly because of the different methodology used in comparison to the kerosene SST.
More data regarding the baseline LH_2 SST, such as a more detailed mass breakdown and a drag polar in cruise can be found in Appendix A.3.

4.3. LH_2 SST with New Engines

After the definition of the baseline LH_2 SST, possible parametric studies to further shorten the fuselage length and therefore enable operability of an LH_2 SST were considered. Since the goal of this study is to evaluate LH_2 SSTs which have the same TLARs compared to the Concorde, and major configurative changes are also out of the scope of this paper, studies in this regard were not considered. However, an interesting parametric study is to replace the Olympus 593 engines with a new engine, which could enable savings in fuel consumption and also possibly in propulsion mass. For this purpose, the data of the ETU-Phoenix engine designed by [49] is used for the rubber engine sizing. This report won the student engine design competition by the American Institute of Aeronautics and Astronautics (AIAA) in 2020-2021. Compared to the Olympus 593 engine, this engine has a 23% lower TSFC alongside being 20% lighter. The resulting LH_2 SST with new engines is presented and compared to the baseline LH_2 SST in this section.
FIG 11 shows a comparison of top and side views and TAB 4 shows selected aircraft parameters of the baseline LH_2 SST and the LH_2 SST with new engines.

FIG 11. Comparison of top and side views of baseline LH_2 SST and LH_2 SST with new engines

TAB 4. Comparison of selected aircraft parameters between the baseline LH_2 SST and the LH_2 SST with new engines

Name	Baseline LH_2 SST	LH_2 SST with new engines	Change
MTOM [kg]	$189,434$	$154,457$	-18%
OEM [kg]	$132,083$	$106,980$	-19%
MLM [kg]	$157,230$	$128,199$	-18%
S_{ref} [m^2]	511	414	-19%
Fuselage length [m]	89.0	72.7	-18%
C_{D0} in cruise [-]	0.0125	0.0178	42%
L/D in cruise [-]	6.51	5.24	-20%
Trip fuel [kg]	$35,591$	$28,099$	-21%
Trip energy [MJ]	$4.27 \cdot 10^9$	$3.37 \cdot 10^9$	-21%
W/S at take-off [N m^{-2}]	$3,637$	$3,661$	1%
T/W at take-off [-]	0.57	0.70	23%

The new engines have a substantial impact on the whole aircraft. Due to the lower TSFC and lower propulsion mass, all other masses are also reduced considerably due to the related snowball effects. Therefore, the wing area can be reduced while the wing loading is kept almost constant. The desired effect of the fuel mass reduction on the fuselage length is achieved, which is reduced to 72.7 m. However, this reduction in fuselage length leads to a significant increase in zero-lift drag, especially wave drag, since the fineness of the fuselage is reduced. The high drag is also reflected in the high thrust-to-weight ratio required to keep the same Mach number and service ceiling. Regardless of the very high zero-lift drag (42% higher) and low L/D in cruise (20% lower), the trip energy consumption of the LH_2 SST with the new engines is reduced to an amount similar to the

kerosene SST. This implies that the total energy consumption can be further reduced with configurative measures to improve aerodynamic performance.
A breakdown of the supersonic zero-lift drag areas ($C_{D0} \cdot S_{ref}$) of both aircraft provides more insight into the influences on drag. FIG 12 shows such a comparison. The zero-lift drag areas are closely tied to the wetted areas of each component. The reduction of the zero-lift drag areas of the wing and fuselage, as well as the increase in the propulsion and vertical tail zero-lift drag areas are hence in line with the expectations. However, as previously mentioned, the increase in supersonic wave drag is substantial, leading to the low supersonic L/D of the whole configuration. Configurative measures to reduce the supersonic wave drag could be an increase of the fuselage fineness up to the required maximum fuselage length of 80 m and a careful wing-fuselage shaping to minimize the gradient of cross-sectional area change.

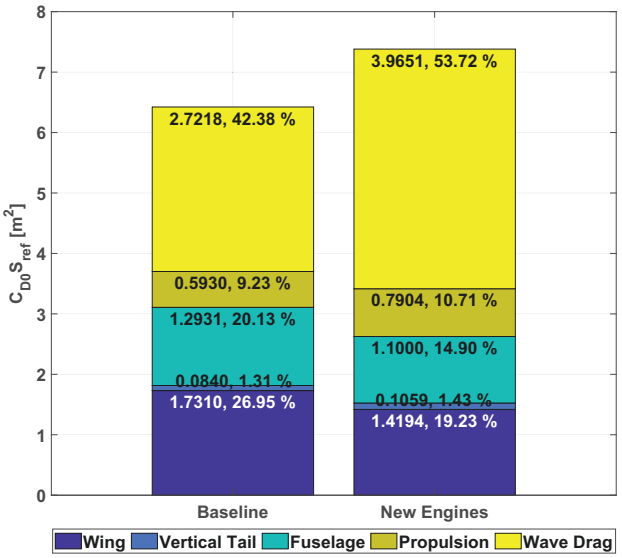

FIG 12. Comparison of supersonic zero-lift drag breakdowns of baseline LH_2 SST and LH_2 SST with new engines

5. CONCLUSION & FUTURE WORK

The aircraft design environment ADEBO was successfully extended for SST design, alongside further modifications for the capability of using LH_2 as the primary energy source. The methodologies used to estimate aircraft characteristics of an SST were validated with a kerosene SST design, which closely matched the Concorde. Using this aircraft as a reference, a baseline LH_2 SST was designed to the same requirements. Options for possible parametric studies were introduced and discussed, since the fuselage length of this LH_2 SST was too long for operational requirements. As the final result, an LH_2 SST with modernized engines was presented, which achieved the desired specifications.
However, this aircraft is not at its optimum regarding many aspects. The lift-to-drag ratio of 5.24 in cruise is in dire need of improvement. To show the true potential of a future LH_2 SST design, further configurative changes are needed, such as a wing planform optimized to the fuselage, so as to minimize the gradient of cross-sectional area change, and therefore supersonic wave drag. Since the requirement of a maximal total length of 80 m is not yet met, a fuselage design with a higher fineness ratio could also be considered. Alongside these changes, LH_2 tanks produced of carbon fiber reinforced polymer (CFRP) can be used instead of the aluminum design currently implemented in this study, reducing the overall mass of the proposed aircraft further.
Even with an optimized LH_2 SST, further open questions regarding the future of such a design remain. For example, the problem of sonic booms associated with supersonic flight is not addressed in this study. For this purpose, the SST design schedule in ADEBO could be extended with methods to estimate and evaluate the acoustic characteristics of the proposed aircraft. Combining the high surface temperatures associated with supersonic flight and very low temperatures of LH_2 also has to be investigated further, with creating synergies from both effects as the focus. Another open question is the evaluation of the climate impact of these SST aircraft. Although LH_2 combustion is CO_2-neutral, it would still lead to the release of a large amount of water vapor at high altitudes, which may contribute significantly to the climate impact via the depletion of the ozone layer [50]. Therefore, a climate impact assessment method, which is compatible with the peculiarities of supersonic flight, should be implemented in the future.

Contact address:

barlas.tuerkyilmaz@tum.de

References

[1] IATA. Global Outlook for Air Transport: Sustained Recovery Amidst Strong Headwinds, 2022. https://www.iata.org/en/iata-repository/publications/economic-reports/global-outlook-for-air-transport---december-2022/.

[2] ICAO. Resolution A41-21, 2022. https://www.icao.int/environmental-protection/Documents/Assembly/Resolution_A41-21_Climate_change.pdf.

[3] ATAG. Net Zero 2050 Declaration, 2022. https://aviationbenefits.org/media/167501/atag-net-zero-2050-declaration.pdf.

[4] S. Herbst. *Development of an Aircraft Design Environment Using an Object-Oriented Data Model in MATLAB*. Dissertation, Technical University of Munich, Munich, 2018.

[5] J. Forestier, P. Lecomte, and P. Poisson-Quinton. Supersonic Air Transport Programs in the 60's. In *Proceedings of the European Symposium on Future Supersonic Hypersonic Transportation Systems*, pages 14–29, 1989.

[6] G. D. Brewer. Advanced Supersonic Technology Concept Study - Hydrogen Fueled Configuration: Final Report, 1974. NASA CR-114718.

[7] Tatsunori Yuhara and Kenichi Rinoie. Feasibility Study of Hydrogen Fueled Supersonic Transport. *AEROSPACE TECHNOLOGY JAPAN, THE JAPAN SOCIETY FOR AERONAUTICAL AND SPACE SCIENCES*, 9(0):29–35, 2010. DOI: 10.2322/astj.9.29.

[8] Tatsunori Yuhara and Kenichi Rinoie. Conceptual Design Study on LH2 Supersonic Transport for the 2030-2035 Time Frame. In *50th AIAA Aerospace Sciences Meeting including the New Horizons Forum and Aerospace Exposition*, Reston, Virginia, 2012. American Institute of Aeronautics and Astronautics. ISBN: 978-1-60086-936-5. DOI: 10.2514/6.2012-23.

[9] Tatsunori Yuhara and Kenichi Rinoie. Multi-Point Optimization Study of Hydrogen-Fueled, Low-Boom Supersonic Transport. *Aerospace Technology Japan (Transactions of the Japan Society for Aeronautical*

and Space Sciences, Aerospace Technology Japan), 10(0):33–42, 2012. DOI: 10.2322/tastj.10.33.

[10] Tatsunori Yuhara, Kenichi Rinoie, and Y. Makino. Conceptual Design Study on LH2 Fueled Supersonic Transport considering Performance and Environmental Impacts. In *52nd Aerospace Sciences Meeting*, Reston, Virginia, 2014. American Institute of Aeronautics and Astronautics. ISBN: 978-1-62410-256-1. DOI: 10.2514/6.2014-0028.

[11] Tatsunori Yuhara, Yoshikazu Makino, and Kenichi Rinoie. Conceptual Design Study on Liquid Hydrogen-Fueled Supersonic Transport Considering Environmental Impacts. *Journal of Aircraft*, 53(4):1168–1173, 2016. ISSN: 0021-8669. DOI: 10.2514/1.C033369.

[12] L. A. McCullers. Aircraft Configuration Optimization Including Optimized Flight Profiles. In *Proceedings of the Symposium on Recent Experiences in Multidisciplinary Analysis and Optimization*, pages 395–412, 1984.

[13] Timothy MacDonald, Emilio Botero, Julius M. Vegh, Anil Variyar, Juan J. Alonso, Tarik H. Orra, and Carlos R. Da Ilario Silva. SUAVE: An Open-Source Environment Enabling Unconventional Vehicle Designs through Higher Fidelity. In *55th AIAA Aerospace Sciences Meeting*, Reston, Virginia, 2017. American Institute of Aeronautics and Astronautics. ISBN: 978-1-62410-447-3. DOI: 10.2514/6.2017-0234.

[14] D. Strohmeyer and R. Seubert. Improvement of a Preliminary Design and Optimization Program for the Evaluation of Future Aircraft Projects. In *Proceedings of the 7th AIAA/USAF/NASA/ISSMO Symposium on Multidisciplinary Analysis and Optimization*, 1998.

[15] Rainer Seubert. The Preliminary Aircraft Design and Optimization Program for Supersonic Commercial Transport Aircraft PrADO-Sup. In Horst Körner and Reinhard Hilbig, editors, *New Results in Numerical and Experimental Fluid Mechanics*, Notes on Numerical Fluid Mechanics (NNFM), pages 311–318. Vieweg+Teubner Verlag, Wiesbaden, 1997. ISBN: 978-3-322-86575-5.

[16] L. Fornasier. HISSS - A higher-order subsonic/supersonic singularity method for calculating linearized potential flow. In *17th Fluid Dynamics, Plasma Dynamics, and Lasers Conference*, Reston, Virginia, 1984. American Institute of Aeronautics and Astronautics. DOI: 10.2514/6.1984-1646.

[17] Daniel P. Raymer. *Aircraft Design: A Conceptual Approach*. AIAA education series. American Institute of Aeronautics and Astronautics Inc, Reston, Virginia, sixth edition, 2018. ISBN: 9781624104909.

[18] Jan Roskam. *Airplane Design: Part I: Preliminary Sizing of Airplanes*. DARcorporation, Lawrence, Kansas, 1989. ISBN: 9781884885426.

[19] Mark Drela and Harold Youngren. Athena Vortex Lattice - AVL, 2004. Software. Accessed: 26.03.2022. https://web.mit.edu/drela/Public/web/avl/.

[20] Egbert Torenbeek. *Synthesis of Subsonic Airplane Design*. Delft University Press and The Hague : Nijhoff and Hingham, Delft, [reprinted] edition, 1982. ISBN: 9789024727247.

[21] LTH Koordinierungsstelle. *Luftfahrttechnisches Handbuch (LTH): Handbuch Masseanalyse*. W. Sellner, Ingenieurbüro für Flugzeugtechnik, Höhenkirchen-Siegertsbrunn, 2006. www.lth-online.de.

[22] B. Malone and W. H. Mason. Multidisciplinary optimization in aircraft design using analytic technology models. *J Aircraft*, 32(2):431–438, 1995.

[23] Gerard Frawley. *The international directory of civil aircraft, 1999/2000*. Aerospace Publications, Fyshwick, Australia, 1999. ISBN: 9781875671427.

[24] British Airways. Concorde Performance Manual: Part 1, 1996.

[25] Eurocontrol. Aircraft Performance Database - Concorde. Internet Document. Accessed: 27.03.2022. https://contentzone.eurocontrol.int/aircraftperformance/details.aspx?ICAO=CONC&ICAOFilter=CONC.

[26] Denis Howe. *Aircraft Conceptual Design Synthesis*. Professional Engineering Publishing, London, 2000. ISBN: 1860583016.

[27] Egbert Torenbeek. *Essentials of Supersonic Commercial Aircraft Conceptual Design*. Aerospace Series. John Wiley & Sons, Inc., Hoboken, NJ, 1st edition, 2020. ISBN: 9781119667049.

[28] Jan Roskam. *Airplane Design: Part II: Preliminary Configuration Design and Integration of the Propulsion System*. DARcorporation, Lawrence, Kansas, 1989. ISBN: 978-1884885433.

[29] M. Nita and D. Scholz. Estimating the Oswald Factor from Basic Aircraft Geometrical Parameters. *Deutscher Luft- und Raumfahrtkongress 2012*, 2012.

[30] T. Paniszczyn. Prediction of Lift and Aerodynamic Center for Variable Sweep Wings. In *5th Aerospace Sciences Meeting*, Reston, Virginia, 1967. American Institute of Aeronautics and Astronautics. DOI: 10.2514/6.1967-135.

[31] Federal Aviation Administration. Concorde Supersonic Transport Aircraft: Environmental Impact Statement, 1976.

[32] ICAO. Annex 6 to the Convention on International Civil Aviation, 2018. http://www.icscc.org.cn/upload/file/20210603/20210603132536_27477.pdf.

[33] Leland M. Nicolai and Grant E. Carichner. *Fundamentals of Aircraft and Airship Design*. American Institute of Aeronautics and Astronautics, Reston, Virginia, 2010. ISBN: 978-1-60086-751-4. DOI: 10.2514/4.867538.

[34] British Airways. Concorde Flying Manual, Volume IIa, 1979.

[35] Robert A. McDonald and James R. Gloudemans. Open Vehicle Sketch Pad: An Open Source Parametric Geometry and Analysis Tool for Conceptual Aircraft Design. In *AIAA SCITECH 2022 Forum*, Reston, Virginia, 2022. American Institute of Aeronautics and Astronautics. ISBN: 978-1-62410-631-6. DOI: 10.2514/6.2022-0004.

[36] Michael J. Waddington. *Development of an Interactive Wave Drag Capability for the OpenVSP Parametric Geometry Tool*. Master's Thesis, California Polytechnic State University, San Luis Obispo, 2015. DOI: 10.15368/theses.2015.126.

[37] Roy V. Harris. An Analysis and Correlation of Aircraft Wave Drag. 1964. NASA TM X-947.

[38] Werner Staudacher. *Die Beeinflussung von Vorderkantenwirbelsystemen schlanker Tragflügel*. Dissertation, University of Stuttgart, Stuttgart, 1991.

[39] M. Hasenau, S. A. Varga, A. E. Scholz, and M. Hornung. Enhancement of an Aircraft Design Environment for the Design of Fighter Aircraft. 2021.

[40] R. D. Finck. USAF Stability and Control DATCOM, 1978. AFWAL-TR-83-3048.

[41] R. D. McCarty, J. Hord, and H. M. Roder. Selected Properties of Hydrogen (Engineering Design Data), 1981. NBS Monograph 168. https://nvlpubs.nist.gov/nistpubs/Legacy/MONO/nbsmonograph168.pdf.

[42] ASTM. Standard Specification for Aviation Turbine Fuels, 1980.

[43] Kristina Kossarev, Anna Elena Scholz, and Mirko Hornung. Comparative environmental life cycle assessment and operating cost analysis of long-range hydrogen and biofuel fueled transport aircraft. *CEAS Aeronautical Journal*, 14(1):3–28, 2023. ISSN: 1869-5582. DOI: 10.1007/s13272-022-00627-w.

[44] G. Daniel Brewer. *Hydrogen Aircraft Technology*. CRC Press, Boca Raton, FL, 1991. ISBN: 0-8493-5838-8.

[45] J. Steiner. *Umrüstung eines Großraumverkehrsflugzeuges für den Betrieb mit flüssigem Wasserstoff unter Vermeidung konfigurativer Änderungen*. Master's Thesis, Technische Universität Berlin, Berlin, 2001.

[46] David Leney and David Macdonald. *Aérospatiale/BAC Concorde: 1969 onwards (all models); owners' workshop manual; an insight into owning, flying and maintaining the world's first supersonic passenger jet*. Haynes and Haynes North America Inc., Sparkford, Yeovil, Somerset and Newbury Park, Calif., 2010. ISBN: 9781844258185.

[47] Elena Sofia Abbagnato. *Conceptual Design Methodology to Size a Supersonic Passengers Aircraft Using LH2*. Master's Thesis, Politecnico di Torino, Torino, 2021. https://webthesis.biblio.polito.it/18933/1/tesi.pdf.

[48] Clives Leyman. *Case Study by Aerospatiale and British Aerospace on the Concorde*. American Institute of Aeronautics and Astronautics, New York, 1980. ISBN: 978-1-56347-308-1. DOI: 10.2514/4.868122.

[49] Mert Battal Şen, Mustafa Cem Canbaz, Yağız Ataberk Erişti, Deniz Akbulut, Remzi Erdem Barış, Tuna Kök, Muaz Yusuf Tağ, Buğrahan Uysal, and Sıtkı Uslu. ETU-Phoenix: 2020-2021 AIAA Engine Design Competition Candidate - Let's Re-Engine the Concorde!, 2021. https://www.aiaa.org/docs/default-source/uploadedfiles/education-and-careers/university-students/design-competitions/winning-reports---2021-engine-design/1st-place---undergraduate-team---tobb-university-of-economics-and-technology.pdf?sfvrsn=72ee1b4f_2.

[50] Sebastian D. Eastham, Thibaud Fritz, Inés Sanz-Morère, Prakash Prashanth, Florian Allroggen, Ronald G. Prinn, Raymond L. Speth, and Steven R. H. Barrett. Impacts of a near-future supersonic aircraft fleet on atmospheric composition and climate. *Environ. Sci.: Atmos.*, 2:388–403, 2022. DOI: 10.1039/D1EA00081K.

A. APPENDIX

A.1. Design Schedules

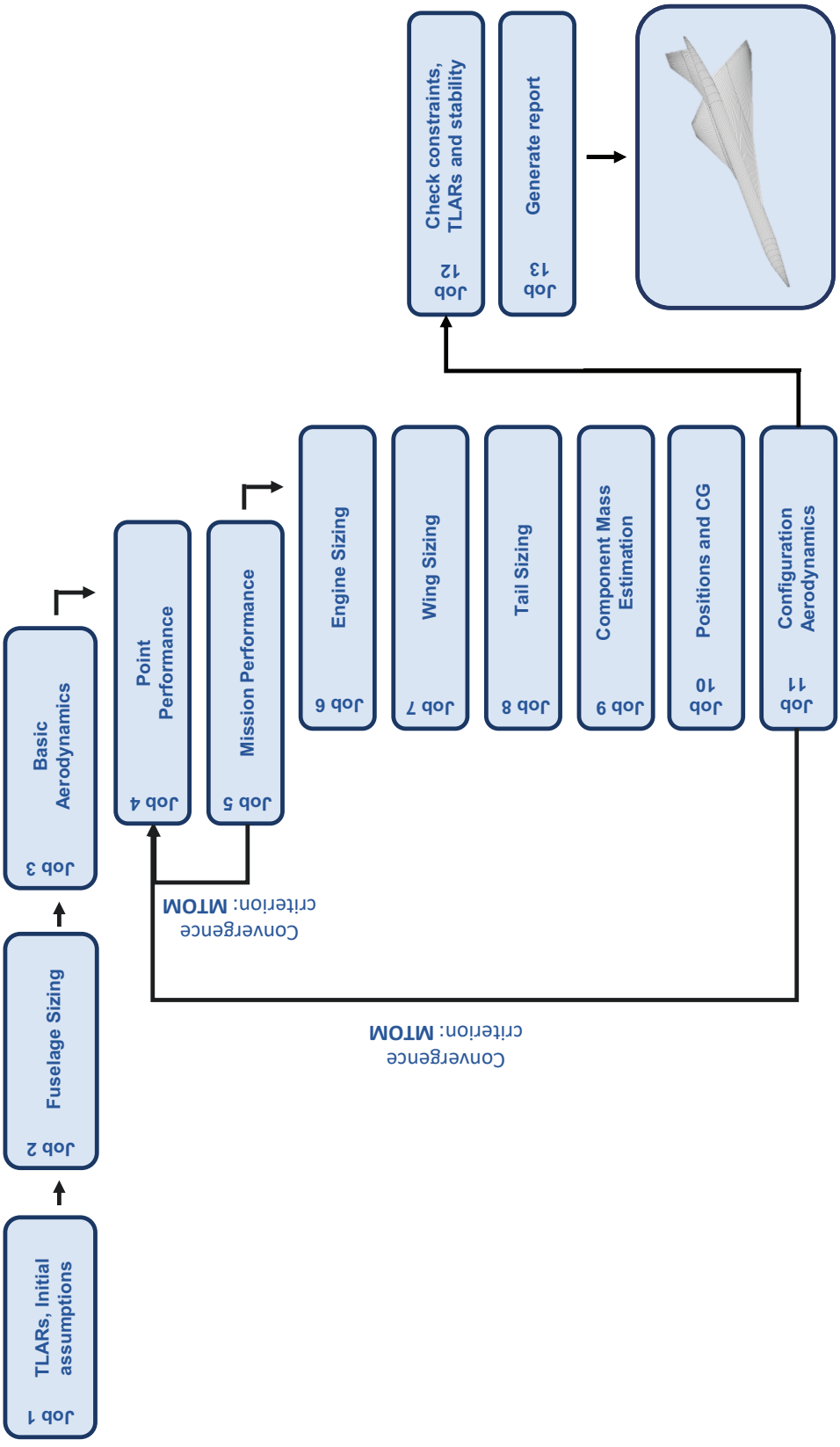

FIG 13. Flowchart of SST design schedule

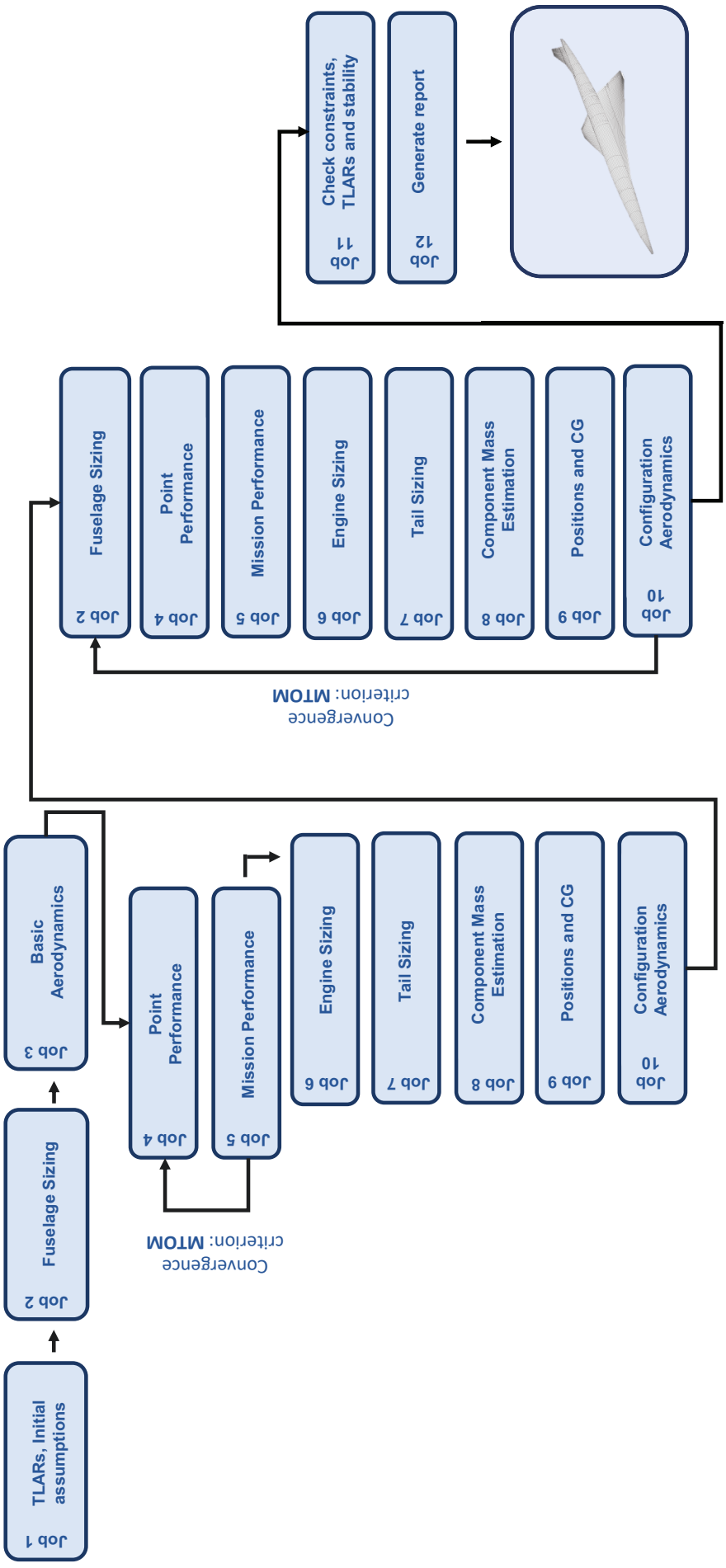

FIG 14. Flowchart of LH_2 SST design schedule

A.2. Kerosene SST

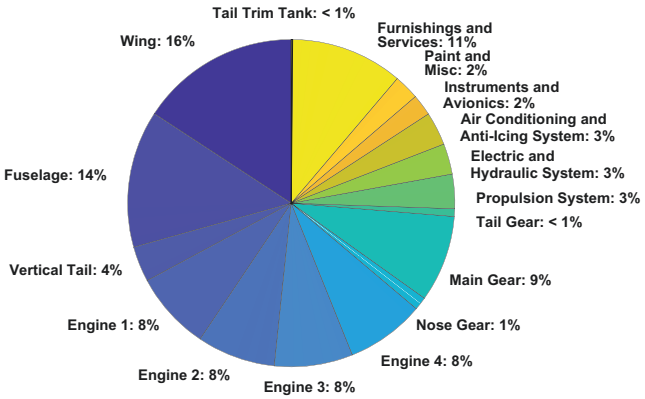

FIG 15. OEM breakdown of kerosene SST

A.3. Baseline LH_2 SST

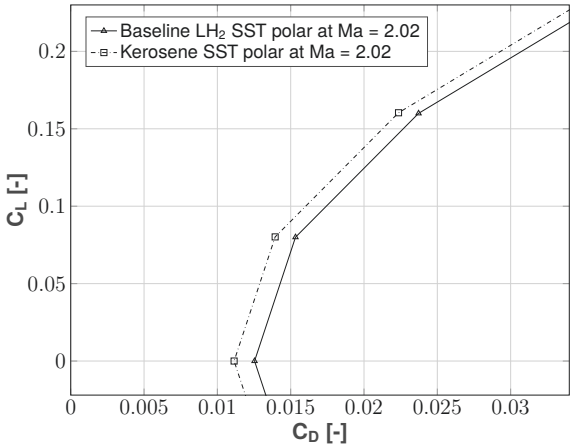

FIG 16. Drag polars of reference kerosene SST and baseline LH_2 SST

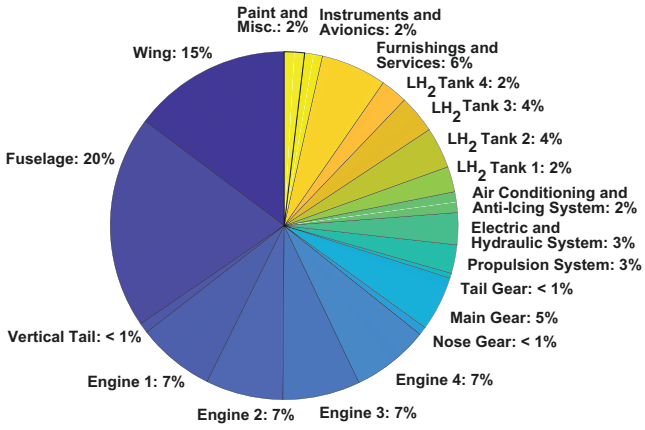

FIG 17. OEM breakdown of baseline LH_2 SST

A.4. LH_2 SST with New Engines

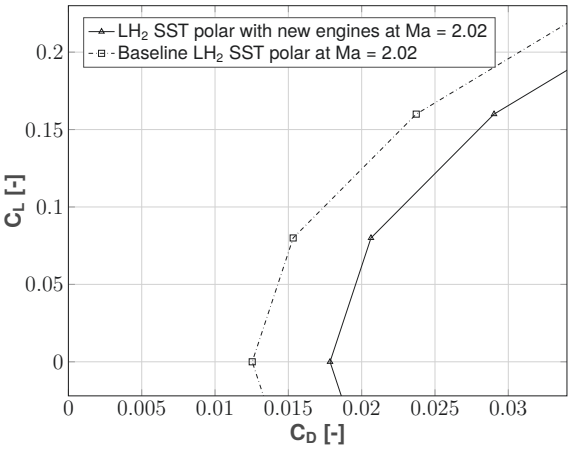

FIG 18. Drag polars of baseline LH_2 SST and LH_2 SST with new engines

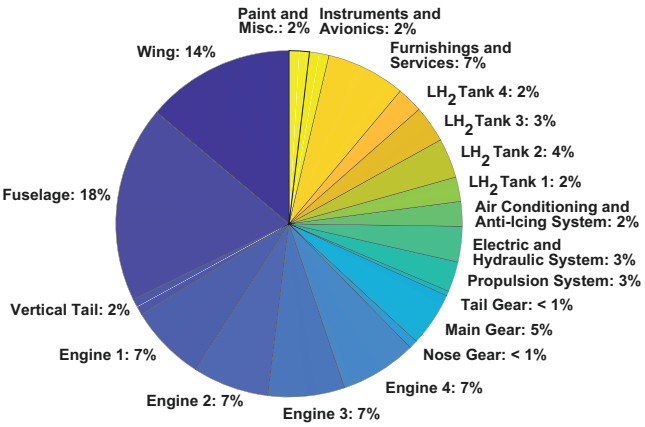

FIG 19. OEM breakdown of LH_2 SST with new engines